

A general estimate for the thermal time-to-steady-state for a solid body suddenly immersed in a fluid stream

Y. MADAY

Laboratoire d'Analyse Numerique, Universite Pierre et Marie Curie, 75252 Paris Cedex 05, France

and

ANTHONY T. PATERA

Department of Mechanical Engineering, Massachusetts Institute of Technology, Cambridge, MA 02139, U.S.A.

(Received 18 July 1991 and in final form 29 April 1992)

Abstract—We present a general, accurate, rigorous upper bound for the time required for the temperature distribution in a solid body suddenly immersed in a flowing fluid stream to reach the steady state. The bound provides a uniform-in-Biot-number estimate that should prove of interest to the heat transfer student and heat transfer practitioner alike: to the former as a succinct summary of the relevant physical phenomena; to the latter as a rough predictive preface to, verification of, and correlation framework for, more precise numerical calculation or experiment.

1. INTRODUCTION

THE PROBLEM of heat transfer in a solid body suddenly immersed in a flowing fluid stream arises in numerous important applications. In most instances, the single quantity of greatest interest is the time required for the body to reach a steady state, that is, the time required for the body to equilibrate to the far-field temperature of the fluid environment.

Although in certain limits the time-constant problem can be treated analytically, these estimates are often imprecise; furthermore, *uniform* estimates over all parameter values are conspicuously absent. In this paper we derive a rigorous, accurate, uniform-in-Biot-number upper bound for the time required for the temperature distribution to reach the steady state. The bound should prove of interest to the heat transfer student and heat transfer practitioner alike: to the former as a succinct summary of the relevant physical phenomena; to the latter as a rough predictive preface to, verification of, and correlation framework for, subsequent precise numerical calculation or experiment.

The outline of this paper is as follows. In Section 2 we state the governing equations, and formally define the equilibration time constant. In Section 3 we briefly survey standard procedures for estimating the time constant. In Section 4 we present our new bound. Lastly, in Section 5, we present numerical results for a simple illustrative example.

2. PROBLEM STATEMENT

2.1. Governing equations

We consider the 'dunking' problem of a solid body with domain Ω , at initial temperature $T_i(\mathbf{x})$, suddenly placed at time $t = 0$ in a flowing fluid medium characterized by a constant-in-time and constant-in-space heat transfer coefficient h . The temperature distribution in the body, $T(\mathbf{x}, t)$, is governed by the standard heat equation

$$\rho c \frac{\partial T}{\partial t} = k \nabla^2 T + \dot{q} \quad \text{in } \Omega \quad (1)$$

$$-k \nabla T \cdot \hat{\mathbf{n}} = h(T - T_\infty) \quad \text{on } \partial\Omega \quad (2)$$

$$T(\mathbf{x}, t = 0) = T_i(\mathbf{x}) \quad \text{in } \Omega \quad (3)$$

where t is time, \mathbf{x} a point in Ω , ρc the (assumed-constant) volumetric specific heat of the body, k the (assumed-constant) conductivity of the body, $\dot{q}(\mathbf{x})$ the constant-in-time volumetric heat generation, $\hat{\mathbf{n}}$ the outward normal on the body surface $\partial\Omega$, and T_∞ the assumed-constant temperature of the fluid far from the solid body. We note that any result derived from equations (1)–(3) is only as accurate as the value and constancy of h ; conjugate calculations are required to improve the situation, albeit at considerable expense.

The situation is depicted in Fig. 1. Although for purposes of illustration we shall consider primarily

NOMENCLATURE			
a	characteristic length scale	Γ_1^k, Γ_0^k	inner and outer boundaries of the k th covering rectangle
Bi	Biot number	ε	degree of steady-state
c	specific heat	η_B^k, η_T^k	functions describing k th covering rectangle
C_1, C_2, C'_1, C'_2	constants depending only on geometry	θ	non-dimensional temperature perturbation
d	bound on η extent of all covering rectangles	θ^k	non-dimensional temperature perturbation in local coordinates in k th covering rectangle
d^k	bound on η extent of k th covering rectangle	Θ	non-dimensional steady-state temperature
ds	surface (line) element	(ξ, η)	local coordinates in covering rectangles
$d\mathbf{x}$	volume (area) element	Ξ	non-dimensional heat generation
D^k	intersection of k th covering rectangle with body domain	ρ	density
h	heat transfer coefficient	τ	time-to-steady-state in $L^2(\Omega)$ norm
$H^1(\Omega), H_0^1(\Omega)$	Sobolev spaces	τ_x	time-to-steady-state in L^∞ norm
k	thermal conductivity	Φ	non-dimensional temperature
l^k	ξ extent of k th covering rectangle	χ	non-dimensional eigenfunction
L	length scale in example	ψ	non-dimensional minimizing eigenfunction
$L^2(\Omega)$	Sobolev space	Ω^k	domain of k th covering rectangle
$\hat{\mathbf{n}}$	outward normal	Ω	domain.
\dot{q}	volumetric heat generation	Other symbols	
R	Rayleigh quotient	$(\cdot)_i$	initial
t	time	$(\cdot)_{LB}$	lower bound
T	temperature	$(\cdot)_{UB}$	upper bound
\bar{T}_i	average initial temperature	$(\cdot)^*$	embedding
T_∞	fluid temperature at infinity	$(\bar{\cdot})$	non-dimensional
\mathbf{x}	space coordinate, (x, y) .	$\partial\Omega$	domain boundary.
Greek symbols			
α	thermal diffusivity		
β	parameter in bound construction		
γ	non-dimensional minimum eigenvalue		

the two-dimensional case, $\mathbf{x} = (x, y)$, our results will apply to three space dimensions as well.

2.2. Non-dimensionalization

Let a be a characteristic length of the body which will be made more precise as the analysis proceeds. The resulting non-dimensional domain and domain boundary will be denoted $\tilde{\Omega}$ and $\partial\tilde{\Omega}$, respectively. For the time scale we then use a^2/α , where α is the thermal diffusivity, $\alpha = k/\rho c$. Lastly, as a temperature scale we choose the average initial temperature

$$\bar{T}_i - T_\infty = \left\{ \int_{\Omega} (T_i(\mathbf{x}) - T_\infty)^2 d\mathbf{x} / \int_{\Omega} d\mathbf{x} \right\}^{1/2}. \quad (4)$$

We then define the non-dimensional variables $\Phi = (T - T_\infty)/(\bar{T}_i - T_\infty)$, $\tilde{t} = \alpha t/a^2$, $\tilde{\mathbf{x}} = \mathbf{x}/a$, $\Xi = \dot{q}a^2/k(\bar{T}_i - T_\infty)$, and $Bi = ha/k$, in terms of which equations (1)–(3) can be written in non-dimensional form as

$$\frac{\partial\Phi}{\partial\tilde{t}} = \tilde{\nabla}^2\Phi + \Xi \quad \text{in } \tilde{\Omega} \quad (5)$$

$$-\tilde{\nabla}\Phi \cdot \tilde{\mathbf{n}} = Bi\Phi \quad \text{on } \partial\tilde{\Omega} \quad (6)$$

$$\Phi(\tilde{\mathbf{x}}, \tilde{t} = 0) = \Phi_i(\tilde{\mathbf{x}}) \quad \text{in } \tilde{\Omega} \quad (7)$$

where

$$\int_{\tilde{\Omega}} \Phi_i^2(\tilde{\mathbf{x}}) d\tilde{\mathbf{x}} / \int_{\tilde{\Omega}} d\tilde{\mathbf{x}} = 1 \quad (8)$$

from the definition (4).

Note that if $T_i(\mathbf{x}) = T_\infty$ we need to introduce a modified non-dimensional temperature, $\tilde{\Phi} = \Phi/\Xi$, with initial condition $\tilde{\Phi} = 0$; with this simple change in scaling the remainder of our results remain unchanged.

2.3. Definition of steady-state

We next consider the temperature as the sum of the steady distribution and unsteady deviation

$$\Phi(\tilde{\mathbf{x}}, \tilde{t}) = \Theta(\tilde{\mathbf{x}}) + \theta(\tilde{\mathbf{x}}, \tilde{t}) \quad (9)$$

where

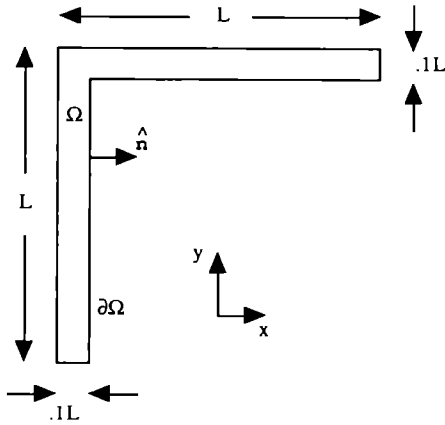


FIG. 1. Example of a 'dunking' problem.

$$\tilde{\nabla}^2 \Theta + \Xi = 0 \quad \text{in } \tilde{\Omega} \quad (10)$$

$$-\tilde{\nabla} \Theta \cdot \tilde{\mathbf{n}} = Bi \Theta \quad \text{on } \partial \tilde{\Omega} \quad (11)$$

and

$$\frac{\partial \theta}{\partial \tilde{t}} = \tilde{\nabla}^2 \theta \quad \text{in } \tilde{\Omega} \quad (12)$$

$$-\nabla \theta \cdot \tilde{\mathbf{n}} = Bi \theta \quad \text{on } \partial \tilde{\Omega} \quad (13)$$

$$\theta(\tilde{\mathbf{x}}, \tilde{t} = 0) = \theta_i(\tilde{\mathbf{x}}) \quad \text{in } \tilde{\Omega} \quad (14)$$

where $\theta_i(\tilde{\mathbf{x}}) = \Phi_i(\tilde{\mathbf{x}}) - \Theta(\tilde{\mathbf{x}})$. Note that if $\Xi = 0$ then $\Theta = 0$.

It is well known that the solution of problem (12)–(14) decays in time. Our interest is to evaluate the *rate* at which the solution goes to zero. In order to be more precise, we need to introduce the norm by which to measure the perturbation. For convenience we shall use the $L^2(\tilde{\Omega})$ -norm, defining the non-dimensional time-constant $\tilde{\tau}(Bi)$ as

$$\begin{aligned} \tilde{\tau}(Bi) &= \max_{\Phi_i, \Xi} \tilde{t} \text{ such that } \left(\int_{\tilde{\Omega}} \theta^2(\tilde{\mathbf{x}}, \tilde{t}) \, d\tilde{\mathbf{x}} \right)^{1/2} \\ &= \varepsilon \left(\int_{\tilde{\Omega}} (\Phi_i(\tilde{\mathbf{x}}) - \Theta(\tilde{\mathbf{x}}))^2 \, d\tilde{\mathbf{x}} \right)^{1/2}. \end{aligned} \quad (15)$$

The dimensional time constant τ is related to the non-dimensional time constant $\tilde{\tau}(Bi)$ by $\tau = \tilde{\tau}a^2/\alpha$. We define $\tilde{\tau}_{UB}(Bi)$ to be a function such that $\tilde{\tau}(Bi) \leq \tilde{\tau}_{UB}(Bi)$ for all Bi .

The choice of ε in (15) determines the 'degree of steady-state' that is required. In the case where Ξ is non-zero, some estimate of Θ is required (for example, based on simple resistance concepts) if $\tilde{\tau}(Bi)$ is to be an *absolute* measure. Note that in the common case in which there is no heat source, $\Xi = 0$, and the initial temperature is uniform, $T_i = \tilde{T}_i$, (15) simply requires that the L^2 -average of $T - T_\infty$ be reduced to ε of $|\tilde{T}_i - T_\infty|$.

It will be of value to express $\tilde{\tau}(Bi)$ in somewhat less abstract form. In particular, we note that $\tilde{\tau}(Bi)$ is defined for a particular body as the *maximum* equi-

libration time over all possible $\Phi_i(\tilde{\mathbf{x}})$ and $\Xi(\tilde{\mathbf{x}})$, and thus $\tilde{\tau}(Bi) = -\ln \varepsilon / \gamma(Bi)$, where $\gamma(Bi) = -\lambda_{\min}$, and λ_{\min} is the minimum eigenvalue of the (non-dimensional) negative-definite eigenproblem

$$\tilde{\nabla}^2 \chi = \lambda \chi \quad \text{in } \tilde{\Omega} \quad (16)$$

$$-\tilde{\nabla} \chi \cdot \tilde{\mathbf{n}} = Bi \chi \quad \text{on } \partial \tilde{\Omega}. \quad (17)$$

As defined, $\tilde{\tau}(Bi)$ is already an upper bound over all initial conditions (Φ_i and Ξ); we reserve the term $\tilde{\tau}_{UB}(Bi)$ for upper bounds of this upper bound, that is, $\tilde{\tau}_{UB}(Bi) = -\ln \varepsilon / \gamma_{LB}(Bi)$, where $\gamma_{LB}(Bi) < \gamma(Bi)$. From (16) and (17) we remark that

$$\begin{aligned} \gamma(Bi) &= \min_{\chi \in H^1(\tilde{\Omega})} R(\chi, Bi) \\ &= \frac{\left\{ Bi \int_{\partial \tilde{\Omega}} \chi^2 \, d\tilde{s} + \int_{\tilde{\Omega}} \tilde{\nabla} \chi \cdot \tilde{\nabla} \chi \, d\tilde{\mathbf{x}} \right\}}{\int_{\tilde{\Omega}} \chi^2 \, d\tilde{\mathbf{x}}} \end{aligned} \quad (18)$$

which is simply the Rayleigh quotient associated with our eigenproblem. The minimizing eigenfunction associated with $\gamma(Bi)$ will be denoted $\psi(Bi)$, that is, $\gamma(Bi) = R(\psi(Bi), Bi)$. Here $\int_{\partial \tilde{\Omega}} \cdot \, d\tilde{s}$ represents the surface (line in two space dimensions) integral over $\partial \tilde{\Omega}$, and $H^1(\tilde{\Omega}) = \{\tilde{v} | \tilde{v} \in L^2(\tilde{\Omega}), \tilde{\nabla} \tilde{v} \in L^2(\tilde{\Omega})\}$.

The Rayleigh quotient result can be arrived at by energy arguments as well: we multiply (12) by θ , perform integration by parts on the right-hand side, and employ (13) on the resulting boundary terms to give

$$\begin{aligned} \frac{1}{2} \frac{d}{d\tilde{t}} \left(\int_{\tilde{\Omega}} \theta^2 \, d\tilde{\mathbf{x}} \right) &= -Bi \int_{\partial \tilde{\Omega}} \theta^2 \, d\tilde{s} \\ &\quad - \int_{\tilde{\Omega}} \tilde{\nabla} \theta \cdot \tilde{\nabla} \theta \, d\tilde{\mathbf{x}}. \end{aligned} \quad (19)$$

It follows that

$$\frac{d}{d\tilde{t}} \int_{\tilde{\Omega}} \theta^2 \, d\tilde{\mathbf{x}} \leq -2\gamma(Bi) \int_{\tilde{\Omega}} \theta^2 \, d\tilde{\mathbf{x}} \quad (20)$$

from which we conclude that

$$\begin{aligned} \left(\int_{\tilde{\Omega}} \theta^2 \, d\tilde{\mathbf{x}} \right)^{1/2} \\ \leq \left(\int_{\tilde{\Omega}} (\Phi_i(\tilde{\mathbf{x}}) - \Theta(\tilde{\mathbf{x}}))^2 \, d\tilde{\mathbf{x}} \right)^{1/2} e^{-\gamma(Bi)\tilde{t}} \end{aligned} \quad (21)$$

and that an upper bound for time-to-steady-state can thus be found from

$$\tilde{\tau}_{UB} = \frac{-\ln \varepsilon}{\gamma_{LB}(Bi)}. \quad (22)$$

It now remains to find a sharp $\gamma_{LB}(Bi)$.

3. PRELIMINARY ANALYSIS

We first consider the low-*Bi* limit. It is immediately apparent from classical heat transfer considerations [1-3] that for $Bi = ha/k \ll 1$

$$\tau \sim -\ln \varepsilon \left(C_1 \frac{\rho ca}{h} \right), \quad Bi \rightarrow 0 \quad (23)$$

(or $\bar{\tau} \sim -\ln \varepsilon(C_1/Bi)$). This can readily be motivated by considering the semi-infinite body conduction solution; in particular, for $Bi \ll 1$, the conduction penetration time a^2/α is small compared to the surface temperature rise time, $k^2/h^2\alpha$, thereby permitting a lumped approximation, $T(t)$, within Ω . Equivalently, for $Bi \ll 1$ the internal conduction resistance is much smaller than the convective resistance. It is simple to show that $C_1 a = |\Omega|/|\partial\Omega|$, where $|\Omega|$ is the volume of the body and $|\partial\Omega|$ is the surface area. This result can also be obtained directly from our Rayleigh quotient (18) by noting that as $Bi \rightarrow 0$, $\psi = \text{const.}$ is the minimizer.

We next consider the high-*Bi* limit. In this case the surface temperature rise time is very small compared to the penetration time (or equivalently the resistance is primarily internal except for very short times), and the time-to-steady-state is then independent of the heat transfer coefficient

$$\tau \sim -\ln \varepsilon(C_2 a^2/\alpha), \quad Bi \rightarrow \infty \quad (24)$$

(or $\bar{\tau} \sim -\ln \varepsilon(C_2)$). The constant C_2 can be estimated by returning to our Rayleigh quotient, and noting that, for large *Bi*, (17) is replaced by $\chi = 0$ on $\partial\tilde{\Omega}$, and thus minimization in (18) is over $\chi \in H_0^1(\tilde{\Omega})$, where $H_0^1(\tilde{\Omega}) = \{\chi | \chi \in H^1(\tilde{\Omega}), \chi|_{\partial\tilde{\Omega}} = 0\}$. The first integral in (18) now vanishes, as $\chi|_{\partial\tilde{\Omega}} = 0$, and we thus arrive at

$$\frac{1}{C_2} = \gamma(\infty) = \min_{\chi \in H_0^1(\tilde{\Omega})} R(\chi, 0) = \frac{\int_{\tilde{\Omega}} \bar{\nabla}\chi \cdot \bar{\nabla}\chi \, d\bar{x}}{\int_{\tilde{\Omega}} \chi^2 \, d\bar{x}} \quad (25)$$

A lower bound can then be obtained for $\gamma(\infty)$ by embedding $\tilde{\Omega}$ in a larger domain $\tilde{\Omega}^*$, $\tilde{\Omega} \subset \tilde{\Omega}^*$, for which the minimum eigenvalue γ^* can be determined more readily; for example, $\tilde{\Omega}^*$ can be chosen as the rectangle of Fig. 2. More precisely, we define γ^* as

$$\gamma^* = \min_{\chi^* \in H_0^1(\tilde{\Omega}^*)} R^*(\chi^*, 0) = \frac{\int_{\tilde{\Omega}^*} \bar{\nabla}\chi^* \cdot \bar{\nabla}\chi^* \, d\bar{x}}{\int_{\tilde{\Omega}^*} \chi^{*2} \, d\bar{x}} \quad (26)$$

and $\hat{\chi}^*$ as $\hat{\chi}^*|_{\tilde{\Omega}} = \psi(\infty)$, $\hat{\chi}^*|_{\text{ext}(\tilde{\Omega})} = 0$. Here $\text{ext}(\tilde{\Omega})$ refers to the complement of $\tilde{\Omega}$ in $\tilde{\Omega}^*$. Since $\hat{\chi}^* \in H_0^1(\tilde{\Omega}^*)$ by virtue of $\psi(\infty)|_{\partial\tilde{\Omega}} = 0$, $\gamma^* \leq R^*(\hat{\chi}^*, 0) = R(\psi(\infty), 0) = \gamma(\infty)$, giving $C_2 = 1/\gamma(\infty) \leq 1/\gamma^*$. Numerical results for this approach will be given in Section 5.

These standard results, though perhaps helpful, are nevertheless highly unsatisfactory. First, the bound-

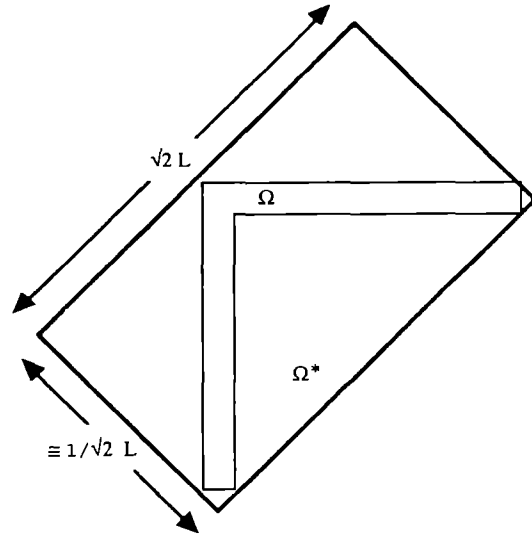


FIG. 2. Example of construction of an upper bound for τ for large *Bi* by the use of variational embedding techniques.

ing techniques are available only for low or high *Bi*, with no uniform estimate possible; the embedding technique of (26) will not extend to finite *Bi* due to the presence of the boundary integral and the nonzero value of χ on $\partial\tilde{\Omega}$. Second, the variational technique (26) is, in practice, not sharp; for example, the embedding shown in Fig. 2 will yield a very poor estimate. Variational techniques, which work quite well for steady conduction estimates [4, 5], are less attractive in the unsteady framework.

A plausible uniform estimate for τ for all Biot numbers is

$$\tau_{UB} = -\ln \varepsilon \left(C_1 \frac{\rho ca}{h} + C_2 \frac{a^2}{\alpha} \right) \quad (27)$$

or, in non-dimensional form

$$\bar{\tau}_{UB}(Bi) = -\ln \varepsilon(C_1/Bi + C_2) \quad (28)$$

as this additive formula correctly represents both limits, $Bi \rightarrow 0$, and $Bi \rightarrow \infty$. Equation (27) can be motivated physically by noting that the time to steady state of a system exhibiting two time scales is dictated by the slower of the two phenomena. We now turn to the new contribution of this paper: a sharp, uniform bound for τ which provides a rigorous construction for formula (27) with explicit values for C_1 and C_2 . Although our methods are mathematical, a simple physical interpretation will result.

4. UNIFORM BOUND FOR $\bar{\tau}$

4.1. Domain decomposition

We shall first break up our domain into parts, then find estimates on the individual building blocks, and subsequently sum to achieve the final $\gamma_{LB}(Bi)$ and hence $\bar{\tau}_{UB}(Bi)$. All results are derived in two space

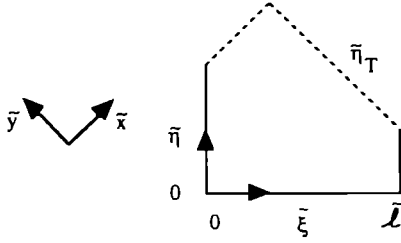


FIG. 3. Example of a generalized rectangle.

dimensions and subsequently extended to three space dimensions. To begin, we define a generalized rectangle to be a standard rectangle save that one side may be curved, as shown in Fig. 3. More specifically, we introduce a local coordinate system $(\xi, \eta) = (\xi/a, \eta/a)$ that defines such a rectangle as $0 < \xi < \bar{l}$, $0 < \eta < \bar{\eta}_T(\xi)$, where $\bar{\eta}_T(\xi)$ is a positive, continuous function of ξ over the interval $]0, \bar{l}[$. We shall also require that the mapping from $(\bar{x}, \bar{y}) = (x/a, y/a)$ to (ξ, η) be shape-preserving, that is, involve only a translation and rotation of (\bar{x}, \bar{y}) . We denote the $\eta = 0$ edge of a generalized rectangle as Γ_0 , and the $\eta = \bar{\eta}_T$ edge as Γ_1 .

We next construct a 'covering' of $\bar{\Omega}$ comprising a set of such rectangles $\bar{\Omega}^k$, $k = 1, \dots, K$, defined by $0 < \xi < \bar{l}^k$, $0 < \eta < \bar{\eta}_T^k(\xi)$ such that

$$\bar{\Omega}^k \cap \bar{\Omega}^l = \emptyset, \quad \text{for } k \neq l \quad (29)$$

$$\bar{\Omega}^k \cap \bar{\Omega} = \bar{D}^k \neq \emptyset, \quad \forall k = 1, \dots, K \quad (30)$$

$$\bar{\Omega} \subset \bigcup_{k=1}^K \bar{\Omega}^k \quad (31)$$

$$\Gamma_0^k \cap \bar{\Omega} = \emptyset, \quad \forall k = 1, \dots, K \quad (32)$$

$$\Gamma_1^k \subset \bar{\Omega}, \quad \forall k = 1, \dots, K \quad (33)$$

$$\bar{\Omega}^k \cap \partial \bar{\Omega} = \bar{\eta}_B^k(\xi), \quad 0 < \xi < \bar{l}^k \quad (34)$$

where $\bar{\eta}_B^k(\xi)$ is a positive continuous function over the entire interval $]0, \bar{l}^k[$. An example of an admissible covering is shown in Fig. 4.

4.2. A bound on $\bar{\Omega}^k$

We now consider a particular $\bar{\Omega}^k$, and derive the result required to form a global bound in the next section. To begin, we write for $\theta^k(\xi, \eta) = \theta(\bar{x}, \bar{y})|_{\bar{\Omega}^k}$

$$\theta^k(\xi, \eta) = \overbrace{\theta^k(\xi, \bar{\eta}_B^k(\xi))}^A + \overbrace{\int_{\bar{\eta}_B^k(\xi)}^{\eta} \frac{\partial \theta^k}{\partial \bar{\eta}'} d\bar{\eta}'}^B \quad (35)$$

If we consider $\theta^k(\xi, \eta) = A + B$, then $(\theta^k)^2(\xi, \eta) = A^2 + 2AB + B^2$; we can then eliminate the AB term in favor of the desired A^2, B^2 terms by using the inequality $2AB \leq \beta A^2 + (1/\beta)B^2$ ($\beta > 0$). This then gives for (35)

$$(\theta^k)^2(\xi, \eta) = (1 + \beta)(\theta^k)^2(\xi, \bar{\eta}_B^k(\xi)) + \left(1 + \frac{1}{\beta}\right) \left(\int_{\bar{\eta}_B^k(\xi)}^{\eta} \frac{\partial \theta^k}{\partial \bar{\eta}'} d\bar{\eta}'\right)^2 \quad (36)$$

The next step is to generate the volume and surface integrals required by (18), giving

$$\begin{aligned} & \int_{\bar{D}^k} (\theta^k)^2(\xi, \eta) d\bar{\eta} d\xi \\ &= (1 + \beta) \int_{\bar{D}^k} (\theta^k)^2(\xi, \bar{\eta}_B^k(\xi)) d\bar{\eta} d\xi \\ &+ \left(1 + \frac{1}{\beta}\right) \int_{\bar{D}^k} \left(\int_{\bar{\eta}_B^k(\xi)}^{\eta} \frac{\partial \theta^k}{\partial \bar{\eta}'} d\bar{\eta}'\right)^2 d\bar{\eta} d\xi \quad (37) \end{aligned}$$

where

$$\int_{\bar{D}^k} \cdot d\bar{\eta} d\xi = \int_0^{\bar{l}^k} \int_{\bar{\eta}_B^k(\xi)}^{\bar{\eta}_T^k(\xi)} \cdot d\bar{\eta} d\xi \quad (38)$$

We first remark that

$$\int_{\bar{D}^k} (\theta^k)^2(\xi, \eta) d\bar{\eta} d\xi = \int_{\bar{D}^k} \theta^2(\bar{x}, \bar{y}) d\bar{x} d\bar{y} \quad (39)$$

by virtue of the unity-Jacobian transformation $(\xi, \eta) \rightarrow (\bar{x}, \bar{y})$. Next, we note that

$$\int_0^{\bar{l}^k} \int_{\bar{\eta}_B^k(\xi)}^{\bar{\eta}_T^k(\xi)} (\theta^k)^2(\xi, \bar{\eta}_B^k(\xi)) d\bar{\eta} d\xi \leq \bar{d}^k \int_{\partial \bar{\Omega}^k \cap \bar{\Omega}^k} \theta^2 d\bar{s} \quad (40)$$

where $\bar{d}^k = \max_{\xi \in]0, \bar{l}^k[} (\bar{\eta}_T^k(\xi) - \bar{\eta}_B^k(\xi))$, and $d\bar{s} = \sqrt{(d\bar{x}^2 + d\bar{y}^2)}$ ($> d\xi$). Lastly, using the Cauchy-Schwarz inequality we reduce the final term in (37) as

$$\begin{aligned} & \int_0^{\bar{l}^k} \int_{\bar{\eta}_B^k(\xi)}^{\bar{\eta}_T^k(\xi)} \left(\int_{\bar{\eta}_B^k(\xi)}^{\eta} \frac{\partial \theta^k}{\partial \bar{\eta}'} d\bar{\eta}'\right)^2 d\bar{\eta} d\xi \\ & \leq \int_0^{\bar{l}^k} \int_{\bar{\eta}_B^k(\xi)}^{\bar{\eta}_T^k(\xi)} \left[(\bar{\eta} - \bar{\eta}_B^k(\xi)) \int_{\bar{\eta}_B^k(\xi)}^{\eta} \left(\frac{\partial \theta^k}{\partial \bar{\eta}'}\right)^2 d\bar{\eta}' \right] d\bar{\eta} d\xi \quad (41) \end{aligned}$$

$$\begin{aligned} & \leq \int_0^{\bar{l}^k} \left\{ \int_{\bar{\eta}_B^k(\xi)}^{\bar{\eta}_T^k(\xi)} \left[\left(\frac{\partial \theta^k}{\partial \bar{\eta}'}\right)^2 + \left(\frac{\partial \theta^k}{\partial \xi}\right)^2 \right] d\bar{\eta}' \right. \\ & \quad \left. \times \int_{\bar{\eta}_B^k(\xi)}^{\bar{\eta}_T^k(\xi)} (\bar{\eta} - \bar{\eta}_B^k(\xi)) d\bar{\eta} \right\} d\xi \quad (42) \\ & \leq \frac{(\bar{d}^k)^2}{2} \int_{\bar{D}^k} \bar{\nabla} \theta \cdot \bar{\nabla} \theta d\bar{x}. \quad (43) \end{aligned}$$

We summarize the result of this section as

$$\begin{aligned} & \int_{\bar{D}^k} \theta^2 d\bar{x} \leq (1 + \beta) \bar{d}^k \int_{\partial \bar{\Omega}^k \cap \bar{\Omega}^k} \theta^2 d\bar{s} \\ & + \left(1 + \frac{1}{\beta}\right) \frac{(\bar{d}^k)^2}{2} \int_{\bar{D}^k} \bar{\nabla} \theta \cdot \bar{\nabla} \theta d\bar{x}. \quad (44) \end{aligned}$$

We now turn to the assembly process.

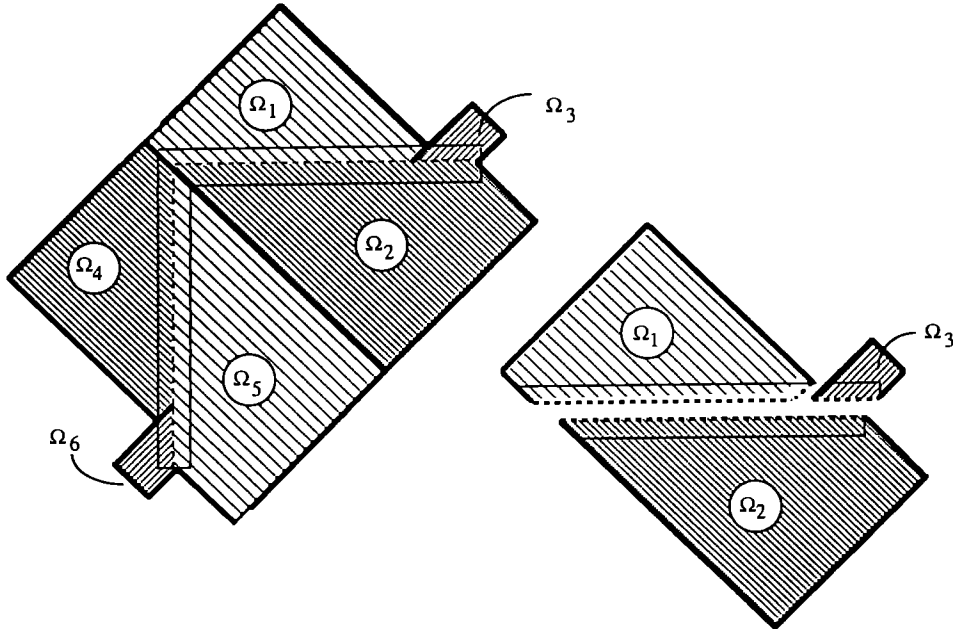


FIG. 4. Admissible covering of the domain Ω of Fig. 1 by $K = 6$ rectangles, $\Omega^1, \dots, \Omega^6$. The shading in each case indicates lines of constant ξ . At bottom right is an exploded view of the covering associated with the right 'wing' of the domain Ω ; dashed lines indicate η_T edges.

4.3. Estimate for $\tilde{\tau}(Bi)$

To begin, we simply sum (44) over all subdomains, giving

$$\sum_{k=1}^K \int_{\Omega^k} \theta^2 d\tilde{\mathbf{x}} \leq (1 + \beta) \sum_{k=1}^K \tilde{d}^k \int_{\partial\Omega \cap \Omega^k} \theta^2 d\tilde{s} + \left(1 + \frac{1}{\beta}\right) \sum_{k=1}^K \frac{(\tilde{d}^k)^2}{2} \int_{\partial\Omega^k} \tilde{\nabla}\theta \cdot \tilde{\nabla}\theta d\tilde{\mathbf{x}}. \quad (45)$$

Defining

$$\tilde{d} = \max_k \tilde{d}^k \quad (46)$$

we then arrive at

$$\int_{\Omega} \theta^2 d\tilde{\mathbf{x}} \leq \tilde{d}(1 + \beta) \int_{\partial\Omega} \theta^2 d\tilde{s} + \frac{\tilde{d}^2}{2} \left(1 + \frac{1}{\beta}\right) \int_{\Omega} \tilde{\nabla}\theta \cdot \tilde{\nabla}\theta d\tilde{\mathbf{x}}. \quad (47)$$

We now remark that, to this point, our length scale a is indeterminate; to simplify what follows we now define $\tilde{d} = 1$, that is

$$a = \max_k \max_{\xi \in [0, l^k]} (\eta_T^k(\xi) - \eta_B^k(\xi)) \quad (48)$$

(note all variables in (48) are dimensional), giving for (47)

$$\int_{\Omega} \theta^2 d\tilde{\mathbf{x}} \leq (1 + \beta) \int_{\partial\Omega} \theta^2 d\tilde{s} + \frac{1}{2} \left(1 + \frac{1}{\beta}\right) \int_{\Omega} \tilde{\nabla}\theta \cdot \tilde{\nabla}\theta d\tilde{\mathbf{x}} \quad (49)$$

or

$$\frac{2}{1 + 1/\beta} \leq \frac{\frac{2(1 + \beta)}{(1 + 1/\beta)} \int_{\partial\Omega} \theta^2 d\tilde{s} + \int_{\Omega} \tilde{\nabla}\theta \cdot \tilde{\nabla}\theta d\tilde{\mathbf{x}}}{\int_{\Omega} \theta^2 d\tilde{\mathbf{x}}} \quad (50)$$

which is now quite close to our Rayleigh quotient (18).

To complete the analysis we now let

$$\frac{2(1 + \beta)}{(1 + 1/\beta)} = Bi \quad (51)$$

which gives (taking the positive solution)

$$\beta = \frac{Bi}{2} \quad (52)$$

yielding

$$\frac{Bi}{1 + Bi/2} \leq \frac{Bi \int_{\partial\Omega} \theta^2 d\tilde{s} + \int_{\Omega} \tilde{\nabla}\theta \cdot \tilde{\nabla}\theta d\tilde{\mathbf{x}}}{\int_{\Omega} \theta^2 d\tilde{\mathbf{x}}} \quad (53)$$

for which we conclude that

$$\gamma_{LB}(Bi) = \frac{Bi}{1 + Bi/2} \quad (54)$$

and

$$\bar{\tau}_{UB}(Bi) = -\ln \varepsilon \left(\frac{1}{Bi} + \frac{1}{2} \right) \quad (55)$$

which is a uniform-in- Bi , and, as we shall see, quite sharp, bound for $\bar{\tau}(Bi)$. The estimate (55) has the form suggested in (28).

For purposes of application we unravel $\bar{\tau}(Bi)$ to arrive at the following dimensional form:

$$\tau_{UB} = -\ln \varepsilon \left(\frac{\rho c a}{h} + \frac{a^2}{2\alpha} \right). \quad (56)$$

It is thus clear that the best bound available from the theory corresponds to that rectangular covering that minimizes a . We now turn to an example which illustrates the physical basis for this optimality, as well as the sharpness of the resulting estimate.

Remark 1. In the case of $\bar{\Omega}$ in three space dimensions the same estimate applies; the only modification to the construction is that one must now consider parallelepipeds with one curved face as opposed to rectangles with one curved side.

Remark 2. In certain cases star-shaped (polar) rather than rectangular (Cartesian) analysis yields a tighter bound; such polar elements can be used in conjunction with rectangles to cover a domain. As the analysis is very similar, and the improvement nominal, we do not discuss this further.

Remark 3. It is possible, though much more difficult, to obtain bounds for $\bar{\tau}_x(Bi)$, defined as

$$\begin{aligned} \bar{\tau}_x(Bi) &= \max_{\Phi, \Xi} \bar{\tau} \text{ such that } \max_{\bar{\mathbf{x}} \in \bar{\Omega}} |\theta(\bar{\mathbf{x}}, \bar{\tau})| \\ &= \varepsilon \max_{\bar{\mathbf{x}} \in \bar{\Omega}} |(\Phi_i - \Theta)(\bar{\mathbf{x}})|. \end{aligned} \quad (57)$$

In general, $\bar{\tau}_x > \bar{\tau}$, however, as $\varepsilon \rightarrow 0$ the two estimates coalesce, indicating that the L^2 estimate may also be used with some confidence in estimating the time at which the maximum deviation from steady-state is very small.

Remark 4. It is very simple to extend our result to other parabolic equations with symmetric negative-definite spatial operators, such as, for example, the Stokes problem of incompressible fluid mechanics.

5. APPLICATION

We consider Ω to be the simple domain shown in Fig. 1. Our decomposition is shown in Fig. 4, which we believe to be an optimal (i.e. a -minimizing) construction ($a = 0.1L/\sqrt{2}$). Note that this a -minimizing solution is not unique: for example, we can readily achieve the same a with only four rectangles by combining rectangles Ω^1 and Ω^4 and rectangles Ω^2 and Ω^5 , respectively.

Taking first the low- Bi limit, we find from (56) $\tau_{UB} = -\ln \varepsilon(0.0707(\rho c L/h))$ compared with the exact low- Bi result (see Section 3) of $\tau = -\ln \varepsilon(0.0475(\rho c L/h))$. Looking now at the high- Bi case, we find from (56) $\tau_{UB} = -\ln \varepsilon(0.0025(L^2/\alpha))$ as compared to the exact solution (found by solving (25) numerically) of $\tau = -\ln \varepsilon(0.00108(L^2/\alpha))$. Had we chosen for large Bi to embed $\Omega \subset \Omega^*$ as in Fig. 2 and use the variational bound of (26) we would obtain $\tau \leq -\ln \varepsilon(0.0405(L^2/\alpha))$, which poorly overestimates the result. (Note that rectangular decomposition *can* result in highly accurate variational estimates as well, in which Dirichlet conditions are imposed at internal boundaries to estimate eigenvalues of the constituent rectangles; unfortunately, the result is not an upper bound for τ .)

The real value of (56) is not only the relatively sharp estimation, but also the uniformity in Biot number:

$$\tau_{UB} = -\ln \varepsilon \left(0.0707 \frac{\rho c L}{h} + 0.0025 \frac{L^2}{\alpha} \right). \quad (58)$$

The physical basis for the uniformity is the fact that, for proper coverings, a accurately reflects the important physical length scales: for low Bi , a can be interpreted as approximately $|\Omega|/|\partial\Omega|$; for high Bi , a can be motivated as the maximum length of the thermal path by which energy is conducted to the boundary.

Acknowledgements—We would like to thank Dr Einar M. Rønquist for performing the numerical calculation of Section 5. This work was supported by the NSF under Grants INT-8914984 and ASC-8806925 and by the ONR and DARPA under Grant N00014-89-J-1610.

REFERENCES

1. J. H. Lienhard, *A Heat Transfer Textbook*. Prentice-Hall, Englewood Cliffs, New Jersey (1987).
2. F. P. Incropera and D. P. Dewitt, *Fundamentals of Heat Transfer*. Wiley, New York (1981).
3. V. S. Arpaci, *Conduction Heat Transfer*. Addison-Wesley, Reading, Massachusetts (1966).
4. H. G. Elrod, Two simple theorems for establishing bounds on the total heat flow in steady-conduction problems with convective boundary conditions. *Trans. ASME J. Heat Transfer* 65–70 (February 1974).
5. M. Magen, B. B. Mikic and A. T. Patera, Bounds for conduction and forced convection heat transfer, *Int. J. Heat Mass Transfer* 31, 1747–1757 (1988).